THE JOURNAL OF BIOLOGICAL CHEMISTRY VOL. 286, NO. 26, pp. 23168–23177, July 1, 2011

Detailed Structural and Quantitative Analysis Reveals the Spatial Organization of the Cell Walls of *in Vivo* Grown *Mycobacterium leprae* and *in Vitro* Grown *Mycobacterium tuberculosis*[*]

Received for publication, December 8, 2010, and in revised form, April 8, 2011 Published, JBC Papers in Press, May 9, 2011, DOI 10.1074/jbc.M110.210534

Suresh Bhamidi, Michael S. Scherman, Victoria Jones, Dean C. Crick, John T. Belisle, Patrick J. Brennan, and Michael R. McNeil[1]

From the Department of Microbiology, Immunology, and Pathology, Colorado State University, Fort Collins, Colorado 80523

The cell wall of mycobacteria consists of an outer membrane, analogous to that of Gram-negative bacteria, attached to the peptidoglycan (PG) via a connecting polysaccharide arabinogalactan (AG). Although the primary structure of these components is fairly well deciphered, issues such as the coverage of the PG layer by covalently attached mycolates in the outer membrane and the spatial details of the mycolic acid attachment to the arabinan have remained unknown. It is also not understood how these components work together to lead to the classical acid-fast staining of mycobacteria. Because the majority of *Mycobacterium tuberculosis* bacteria in established experimental animal infections are acid-fast negative, clearly cell wall changes are occurring. To address both the spatial properties of mycobacterial cell walls and to begin to study the differences between bacteria grown in animals and cultures, the cell walls of *Mycobacterium leprae* grown in armadillos was characterized and compared with that of *M. tuberculosis* grown in culture. Most fundamentally, it was determined that the cell wall of *M. leprae* contained significantly more mycolic acids attached to PG than that of *in vitro* grown *M. tuberculosis* (mycolate:PG ratios of 21:10 *versus* 16:10, respectively). In keeping with this difference, more arabinogalactan (AG) molecules, linking the mycolic acids to PG, were found. Differences in the structures of the AG were also found; the AG of *M. leprae* is smaller than that of *M. tuberculosis,* although the same basic structural motifs are retained.

The hallmark of mycobacteria is their cell wall consisting of a peptidoglycan layer attached to a mycolic acid containing outer membrane via the polysaccharide arabinogalactan. Profound and fundamental questions remain about this architecture, including how division occurs and how molecules, both nutrients and drugs, enter the cell. Although its impermeability is stressed (1), anomalies exist such as the susceptibility of *in vitro* grown *Mycobacterium tuberculosis* to lysozyme at concentrations between 0.1 and 3 mg/ml.[2] Also, the acid fastness of *in vivo* bacteria varies, in a manner dependent upon their growth state (2). Considered together, these phenomena point to the need to understand the cell wall physical spatial organization and how the cell wall changes during *in vivo* growth.

Mycobacterium leprae cannot be cultured *in vitro* and is propagated in nine-banded armadillos (*Dasypus novemcinctus*) (3). In this animal, as in the mouse foot pad model and human lepromatous leprosy, the bacteria grow logarithmically but with a very slow generation time of 12–14 days (4). Although there is a robust humoral response to *M. leprae* in armadillo, it would appear that the immune system does little to slow the growth of the bacteria and that the slow growth rate is an intrinsic property of the highly attenuated *M. leprae*, marked by less than 50% genomic coding capacity (5). This is in contrast to *M. tuberculosis* that presents an initial doubling time in animal models of about 2.4 days (5) until the adaptive immune response is fully activated and stops *M. tuberculosis* bacilli replication (6), although the bacteria are still viable. The nongrowing *M. tuberculosis* is resistant to chemotherapy and to clearing by the immune system. Thus, it is important to study the cell wall barrier of mycobacteria under all of these conditions, and here we begin with a study of *in vivo M. leprae.*

Previous cell wall analyses of *in vivo* grown leprosy bacilli reported the presence of the characteristic mycobacterial cell wall sugars arabinose and galactose and the amino acids diaminopimelic acid (DAP),[3] alanine, and glutamic acid (7, 8). Further analysis of the arabinogalactan and peptidoglycan from *M. leprae* revealed structural similarities with related mycobacterial species (9). Torrelles *et al.* (10) reported that the arabinan architecture of *M. leprae* lipoarabinomannan, an important cell envelope component, is simpler than that of *M. tuberculosis* with a high degree of exposed nonmannosylated capped arabinan termini (10). More recently, it was found that in the case of *M. leprae* peptidoglycan, the muramic acid residues are exclusively *N*-acetylated, unlike *M. tuberculosis* where both *N*-acetylated and *N*-glycosylated versions of muramic acid exist (11). However, a comprehensive and quantitative comparison of the

* This work was supported, in whole or in part, by National Institutes of Health Grants AI-33706 (to M. R. M.), AI049151 (to D. C. C.), and AI018357 (to P. J. B.) from USPHS NIAID. This work was also supported by Grant 42775 from the Bill and Melinda Gates Foundation (to J. T. B. and D. C. C.).

[1] To whom correspondence should be addressed: Dept. of Microbiology, Immunology, and Pathology, Colorado State University, Fort Collins, CO 80523-1682. Tel.: 970-491-1784; Fax: 970-491-1815; E-mail: mmcneil@colostate.edu.

[2] M. S. Scherman and M. R. McNeil, unpublished observation.

[3] The abbreviations used are: DAP, diaminopimelic acid; PG, peptidoglycan; AG, arabinogalactan; mAGP, mycolyl arabinogalactan peptidoglycan complex; $GalNH_2$, galactosaminosyl.

cell wall core of *in vivo* grown *M. leprae versus in vitro* grown *M. tuberculosis* is lacking.

The cell wall core of *in vitro* grown *M. tuberculosis* has been studied in great detail. Analyses of the *O*-alkylated alditols of AG-derived oligosaccharides revealed the following: (i) the attachment of arabinan side chains to a linear galactan chain, with a specific hexaarabinoside at its nonreducing end (12); (ii) the linker disaccharide (Rha-GlcNAc)-P at the reducing end (13) of the entire AG molecule; and (iii) the location of the outer membrane-located mycolyl esters at the nonreducing end of the arabinan (14). The use of a partially purified endo-arabinase from *Mycobacterium smegmatis* that specifically cleaves the α-1,5 linkages allowed released oligoarabinans to be characterized by matrix-assisted laser desorption/ionization-time of flight mass spectrometry (MALDI-TOF) (15, 16) and the realization that two hexaarabinosides are connected to yield an Ara_{17} unit (see Fig. 2). Additionally, the nonessentiality of the arabinogalactan biosynthetic genes in the closely related *Corynebacterium glutamicum* allowed definition of the nature of the attachment of the arabinan to the galactan (17). Finally, a recent report from our group has defined the entire primary structure of the cell wall mycolyl arabinogalactan identifying the location of the attached succinyl residues and re-defining the structure of the interior arabinan chain of *M. tuberculosis* and *M. smegmatis* (16).

Recent cryotomography EM studies (18, 19) unequivocally showed that covalently attached mycolic acids are present as part of a true outer membrane. This observation gives rise to the question of what percentage of the inner leaflet of this outer membrane is composed of mycolic acid esters covalently attached to peptidoglycan via the AG as compared with noncovalently attached lipids, such as the trehalose mycolates that are also located in the outer membrane.

In this study, endo-arabinase digestion coupled with carefully designed methylation and compositional analyses were applied to the cell wall core of *M. leprae* and to the cell wall of *in vitro* grown *M. tuberculosis.* The results lead to a model focusing on the spatial arrangement of the mycolic acids of the two cell wall cores and provide new perspectives on the distinct outer membrane of *Mycobacterium* spp.

EXPERIMENTAL PROCEDURES

Bacterial Cultures—M. leprae was obtained from armadillo livers and spleens as described previously (20). *M. tuberculosis* (H37Rv) and *M. smegmatis* mc^2 155 were grown and harvested as described previously (16).

Preparation of Mycolyl Arabinogalactan Peptidoglycan Cell Wall Core (mAGP)—Mycobacterial cells were disrupted mechanically in 10 mM PBS buffer (pH 8) using a French press (SIM-AMINCO systems) at 1500 p.s.i. followed by centrifuging at 21,000 $\times$ *g* for 30 min. The pellet obtained was suspended in 30 ml of Milli-Q water containing 2% SDS and stirred gently at room temperature overnight. This was followed by centrifugation (25,000 $\times$ *g*) to remove the supernatant. The pellet was suspended in 30 ml of Milli-Q water containing 2% SDS and stirred gently at 100 °C for 1 h, followed by centrifuging at 25,000 $\times$ *g* for 30 min, and the supernatant was removed. The pellet was washed with water (three times) followed by centrifugations as above. After the water washes, the pellet was suspended in 30 ml of 80% acetone/Milli-Q water and centrifuged at 25,000 $\times$ *g* for 20 min to remove SDS. This was again followed by two more water washes. Finally, the material was treated with organic solvents ($CHCl_3$:CH_3OH, 2:1; overnight extraction) to remove any remaining noncovalently attached mycolic acids. The resulting insoluble final pellet was considered as mAGP and is a cell wall with only the covalently attached inner leaflet of the outer membrane.

Analysis of Cell Wall Components—The resulting mAGP (1 mg in the case of both that from *M. leprae* and *M. tuberculosis*) was treated with 2 M TFA (500 μl) for 2 h at 120 °C after adding the internal standards 3-*O*-methyl glucose and α-aminoadipic acid (for sugar and amino acid quantitation, respectively). After cooling down to room temperature, it was extracted twice with 500 μl of $CHCl_3$. The organic phases were pooled, dried under N_2, and processed further for mycolate analysis. The aqueous phase was divided to two equal parts, for sugar and DAP analyses.

Derivatization of Cell Wall Sugars to Alditol Acetates—The aqueous extract obtained after TFA hydrolysis was dried and reduced with $NaBD_4$ (10 mg/ml in 1 M NH_4OH:C_2H_5OH) for 4 h at room temperature. Excess $NaBD_4$ was removed by adding 20 μl of CH_3COOH (glacial acetic acid), and the tubes were dried under N_2, followed by two more CH_3OH washes and subsequent drying steps. The samples were per-acetylated using 100 μl of acetic anhydride and heated for 1 h at 100 °C. After acetylation, samples were cooled to room temperature and extracted with $CHCl_3$:H_2O (1:1), and the $CHCl_3$ layer was dried and analyzed by GC/MS.

GC/MS Analysis of Cell Wall Sugars—GC/MS analyses were carried out using a CP3800 gas chromatograph (Varian Inc., Palo Alto, CA) equipped with an MS320 mass spectrometer. The samples were run on a DB 5 column (30 m $\times$ 0.20 mm inner diameter). The oven temperature was held at 50 °C for 1 min and programmed at 30 °C/min to 150 °C and then programmed at 5 °C/min to 275 °C.

Per-O-methylation of Cell Wall Glycosyl Residues—The mycobacterial cell wall core (mAGP) was subjected to methylation as per Ciucanu and Karek (21). Typically, five pellets of NaOH and 3 ml of anhydrous DMSO were ground using a mortar and a pestle, and the slurry was added to a sample of mAGP, followed by an addition of 500 μl of CH_3I. This mixture was vigorously shaken for 1 h at room temperature. The reaction was quenched with a dropwise addition of 1 ml of water and was extracted three times with 2 ml of $CHCl_3$. The $CHCl_3$ extracts were pooled, again extracted with distilled water, and finally dried under N_2. An aliquot of the methylated sample was subjected to hydrolysis, reduction, and acetylation by the alditol acetate procedure as described above for the identification and quantitation of linked sugars.

Quantitation of Per-O-methylated Sugars—GC/MS analysis of the partially methylated and partially acetylated alditols was used to identify them. The GC/MS conditions were as described earlier for neutral sugar analysis. Quantitation of the different components was achieved using the effective carbon response theory (22). For this, the partially methylated cell wall sugars were run on a GC (Shimazu, Columbia, MD) equipped

with a flame ionization detector. The molar response factors of partially methylated sugars from the effective carbon response theory (22) were then used to calculate the ratios of the variously linked glycosyl residues of the cell wall core.

Analysis of Diaminopimelic Acid—The remaining 50% of the aqueous phase from TFA hydrolysis of mAGP was dried and treated with 6 N HCl at 120 °C for 16 h to release all amino acids, including DAP. The products were derivatized with *n*-propyl chloroformate ("EZ:faast" kit; Phenomenex, Torrance CA) and analyzed by GC/MS. In this procedure, the amino acids are purified after 6 M HCl hydrolysis by cation exchange before derivatization with *n*-propyl chloroformate in the presence of *n*-propyl alcohol. A standard of DAP was prepared in the same fashion; it and the unknown samples contained α-aminoadipic acid as an internal standard.

Analysis of Mycolic Acids—The organic layer of the 2 M TFA-hydrolyzed mAGP contains mycolic acids covalently attached to arabinosyl residues (presumably the α-branched and β-hydroxylated components of the mycolate structure account for the acid stability of the ester (23)). Although the arabinosyl mycolate can be analyzed directly by LC/MS, better sensitivity results after de-esterification. Thus, arabinosylated mycolic acids released by 2 M TFA from the mAGP were subjected to alkaline hydrolysis (24), acidified with HCl, and extracted twice with diethyl ether. The pooled ether fractions were dried under a stream of nitrogen and dissolved in 200 μl of $CHCl_3$:CH_3OH (2:1) for LC/MS analysis. The compound, 1,2-dioleoyl-*sn*-glycerol-3-phosphoethanolamine-*N*-nonadecanoyl, was used as an internal standard for quantitation of mycolates (Avanti Polar Lipids, Alabaster, AL). For a standard, large amounts of pure mycolic acids were prepared from *M. tuberculosis* cells so that they could be weighed.

The ESI/APCI-MS (negative mode) was performed on an Agilent 6220 TOF mass spectrometer equipped with a Multi-Mode source. The HPLC was equipped with an Agilent 1200 binary pump. Two tandemly attached Waters XBridge (C18 2.1 × 150 mm, 5 μM particle size) columns were used for the separation of the mycolic acids. The column temperature was 45 °C. The separation was done using a gradient of 100% solvent A (99% CH_3OH + 1% 500 mM ammonium acetate) to 100% solvent B (79% *n*-propyl alcohol + 20% hexane + 1% 500 mM ammonium acetate) (25). The column eluent was introduced into the multimode source operated in the negative ion mode. The drying gas temperature was 300 °C, and the vaporizer temperature was set at 200 °C. Typically, 5 μl of sample was injected for analysis, with a flow rate of 0.32 ml/min, and the total run time was 45 min. The fragmentor voltage was set to 120 V. The mass spectrum was acquired from *m*/*z* 250 to 3200 Da with a frequency of 1 scan/s. MS data were analyzed using Mass Hunter software (Agilent) and a custom data base of *M. tuberculosis* lipids (40).

To analyze the size of the α chain, the mycolates were subjected to LC/MS/MS (25). An Agilent 6520 qTOF was used for MS/MS analyses of the mycolic acids. The chromatographic setup was similar to the one described above for mycolic acid analysis. Mass spectra were acquired in Auto MS/MS mode with N_2 as a collision gas, and collision energy of 75 eV was used for fragmentation.

Treatment of the Cell Wall Core with Endogenous Arabinase and Purification of Arabinans—mAGP was incubated with a partially purified (15) *M. smegmatis* arabinase at 37 °C for 12 h, followed by extraction with $CHCl_3$:CH_3OH:H_2O (10:10:3) in which, surprisingly, the arabinan is soluble (16). The 10:10:3 extract was dried and extracted with $CHCl_3$:CH_3OH:H_2O (8:4:3); and the aqueous fraction was collected. This fraction was passed through a P-2 column (BioGel, 1 × 25 cm) and eluted with 50 mM sodium acetate buffer (pH 5). The collected fractions were hydrolyzed and derivatized as alditol acetates and further analyzed by GC/MS to identify which fraction contained galactosamine. As in our earlier work, it was observed that the earlier fractions of the P-2 column contained the majority of the galactosamine residues (16). The dried samples from the P-2 column (showing higher arabinan content) were per-*O*-acetylated with 100 μl of acetic anhydride in the presence of 50 μl of pyridine (room temperature, overnight) and were extracted in $CHCl_3$:H_2O (1:1). The $CHCl_3$ layer upon concentration was analyzed by matrix-assisted laser desorption ionization-time of flight mass spectrometry (MALDI-TOF MS) in the positive ion reflector mode on a Bruker Ultraflex MALDI-TOF/TOF mass spectrometer (Bruker Daltonics, Billerica, MA). The sample (1 μl) was mixed with 1 μl of matrix (dihydroxybenzoic acid) at 10 mg/ml in 50% acetonitrile in 0.1% TFA) and allowed to air-dry on the MALDI target plate.

Analysis of Succinates—Succinates from the cell wall core (mAGP) were obtained through octanolysis using 3 N HCl in 1-octanol (99%, 100 μl) at 120 °C for 30 min (16). The resultant octyl succinate derivatives were extracted with 2 ml each of hexane and a supersaturated solution of sodium bicarbonate. The hexane layer was further analyzed by GC/MS with a DB-5 column. The initial temperature of the column was at 60 °C, held for 1 min. The temperature was increased to 330 °C at a rate of 30 °C/min. The retention times were compared with that of standard succinic acid and were further quantified by comparing the area of internal standard glutaric acid (as octyl ester), which was also subjected to octanolysis as per the procedure (16).

RESULTS

Comparative Compositional Analysis of the mAGP of in Vivo Grown M. leprae and in Vitro Grown M. tuberculosis—Crude cell walls (27,000 × *g* pellets after centrifugation of the bacteria broken by a French press) were prepared from *M. leprae* isolated from armadillos and from *M. tuberculosis* grown in culture. These included the entire outer membrane but unfortunately were contaminated with fragments of plasma membrane. Hence the crude cell walls were extracted with chloroform to yield the cell wall core composed only of the covalently attached mycolic acids, arabinogalactan and peptidoglycan (mAGP). The only aspects of the outer membrane remaining were the mycolates covalently attached to the AG·PG complex because all of the free mycolate-containing neutral lipids had been removed.

To obtain compositional data on mAGP from the two mycobacterial species, the glycosyl residues were analyzed as alditol acetates after release by 2 M TFA. DAP, released by 6 M HCl hydrolysis, was analyzed after derivatization with *n*-propyl

chloroformate, and the mycolic acids were measured as free mycolate anions after base hydrolysis (Table 1). All three analyses were done from the same sample rather than using separate aliquots for each analysis to increase the accuracy of the ratios of the different components.

The ratios of DAP, Rha, and mycolate can be used to calculate the ratios of PG:AG:mycolate as shown in Table 1. DAP is used as a marker for PG because it is quantitatively released by the 6 M HCl and not significantly degraded by the acid. It is not possible to accurately quantitate the PG amino sugars due to the fact they are not completely released by 2 M TFA, and the stronger acid conditions required for their hydrolysis also degrades them. Thus, their ratio to Rha is underestimated in Table 1. The component used for AG quantitation is the rhamnosyl residue because one rhamnosyl unit is present per AG chain, and it is released and not degraded by the 2 M TFA. The mycolates are accurately measured due to their efficient release, without degradation, by base.

The data (Table 1) show that compared with *M. tuberculosis*, *M. leprae* mAGP has a 1.3 (20.8/16.4)-fold increase in the amount of mycolic acids and a 2.3 (3.0/1.3)-fold increase in arabinogalactan for a given amount of peptidoglycan. This requires that more mycolic acids be covalently attached to PG and more AG be present to make that attachment. These changes are modeled below.

Comparison of the Mycolates of M. leprae and M. tuberculosis—The mycolic acid amounts shown in Table 1 represent all the different classes obtained by integrating the entire complex mycolate peak in the LC/MS total ion chromatogram and comparing that area with that of an internal standard. Further information on the mycolate species present is also available from the LC/MS analysis. Thus, because the LC/MS was run with high mass resolution, the number of oxygen atoms present per mycolate molecule is readily determined from the exact molecular weights of each mycolate. This allowed the mycolates to be readily assigned to their appropriate class of α, keto, and methoxy. In keeping with the data of others (26), the *M. leprae* mycolates are present as α- and keto-mycolate classes, but the methoxy-mycolates are lacking (Fig. 1*A*). The α- and keto-mycolates were equally distributed (Fig. 1*A*). The α class mycolates with total carbon numbers of 78 and 80 and the keto class of C-83 were most abundant in *M. leprae* (Fig. 1*B*). Tandem mass spectrometry (LC/MS-MS) analysis of the α-mycolate from *M. leprae* (α-78) (Fig. 1*C*) showed that the predominant α chain was C-22; C-24 α chains are also present as originally shown (27). For purposes of comparison, the same data are shown for the mycolates of *in vitro* grown *M. tuberculosis* (Fig. 1, *D–F*); these data are consistent with analyses of others (28, 29). The most notable differences between the mycolates of the two species are the lack of methoxy mycolates in *M. leprae* and the presence of C-22 (with some C-24) α chains in *M. leprae* as compared with C-26 (with some C-24) α chains in *in vitro* grown *M. tuberculosis.*

Analysis of AG—Glycosyl linkage analysis of the AG of *M. leprae* and *M. tuberculosis* as determined by per-*O*-methylation (Table 2) as well as the neutral sugar analysis (Table 1) reflects the lower amounts of galactofuranose and to some extent the arabinofuranose in the *M. leprae* AG compared with *M. tuber-*

TABLE 1
The composition of the cell wall core (mAGP) from *M. tuberculosis* and *M. leprae*

Origin of mAGP	mol % (standard deviation in parentheses[a]) normalized to 1 Rha residue (boldface type)								Macromolecular component ratios[b] (propagated standard deviation in parentheses)				
	Rha	Ara[c]	Gal	GalNAc[d]	Total glycosyl residues in AG	GlcNAc[d]	MurNAc[d]	DAP	Myc	PG[e]	AG	Myc	% substitution of AG with Myc[f]
M. tuberculosis	0.95 (0.05)	53.6 (0.92)	21.3 (0.69)	0.81 (0.05)		2.2 (0.46)	1.91 (0.1)	7.3 (0.37)	12.0 (1.0)	10	1.3 (0.03)	16.4 (2.2)	79 (9.6)
	1	**54**	**23**	**0.9**	**79**	**2.3**	**2.0**	**7.7**	**12.7**				
M. leprae	1.39 (0.08)	62 (1.3)	18 (2.4)	0.7 (0.2)		2.0 (0.6)	1.7 (0.6)	4.6 (0.4)	9.4 (1)	10	3.0 (0.23)	20.8 (4.4)	42 (2.7)
	1	**45**	**13**	**0.5**	**59.5**	**1.4**	**1.2**	**3.3**	**6.7**				

[a] Four separate samples of mAGP from *M. tuberculosis* and *M. leprae* were analyzed. The ratios are the average from these four analyses, and the standard deviation is calculated from them. The amount of mAGP from both sources used for analyses was approximately 1 mg.
[b] These ratios are calculated from the DAP, Rha, and Myc values; see text for justification.
[c] The total number of Ara residues includes those attached to the mycolic acids and not liberated by acid hydrolysis.
[d] GlcNAc, $GalNH_2$, and MurNAc cannot be accurately quantitated due to the fact that acid conditions either fail to fully hydrolyze them or stronger conditions degrade them after liberation. Thus, these values are not used for further calculations.
[e] The PG is chosen to include 10 disaccharide/peptide repeating units for clarity of ratios. There is always one DAP per PG repeating unit.
[f] Data were calculated based on the ratio of Myc to AG recognizing that 16 mycolic acids per AG is fully mycolylated AG.

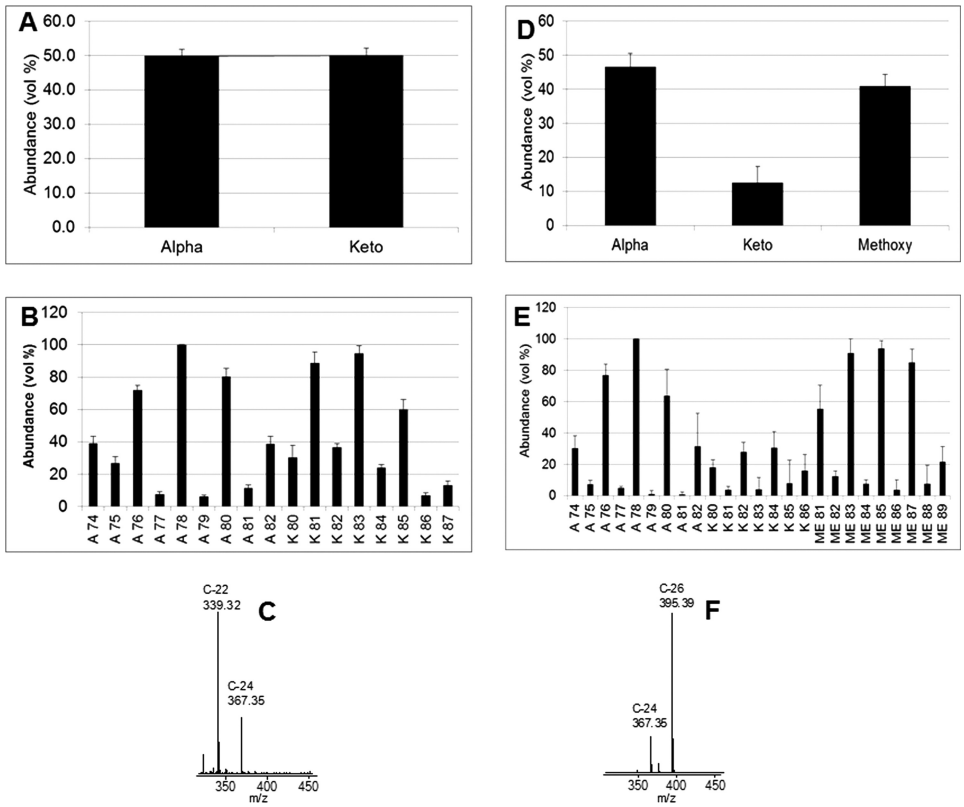

FIGURE 1. *A,* relative abundance of the two major classes of mycolic acids, α and keto, present in *M. leprae* bacteria. *B,* chain length distribution of these *M. leprae* mycolic acids. *C,* LC/MS-MS analysis showing that the C-22 α chain is predominant in the mycolic acids of *M. leprae* (spectrum shown is from the α-78 where *m/z* 1136 was targeted). *D,* relative abundance of the three major classes of mycolic acids, α, methoxy, and keto, present in *M. tuberculosis* bacteria. *E,* chain length distribution of these *M. tuberculosis* mycolic acids. *F,* LC/MS-MS analysis showing that the C-26 α chain is predominant in the mycolic acids of *M. tuberculosis* (spectrum shown is from the α-78 where *m/z* 1136 was targeted). Four separate samples were analyzed, and the values presented here are the average of those; the standard deviation is shown on the graphs.

TABLE 2

Glycosyl linkage composition of *M. tuberculosis* and *M. leprae* cell walls

Four separate samples of mAGP from *M. tuberculosis* and *M. leprae* were analyzed. The ratios are the average from these four analyses, and the standard deviation is calculated from them.

Glycosyl residue	*M. leprae*[a] (mol/59 mol)	Theoretical 2 Ara_{22} units and 1 Gal_{14} unit	*M. tuberculosis*[b] (mol/79 mol)	Theoretical 2 Ara_{26} units and 1 Gal_{22} unit
T-Ara*f*	5 (0.09)	8.0	7 (0.25)	8
2-Ara*f*	5 (0.27)	8.0	7 (0.38)	8
5-Ara*f*	25 (0.37)	22	29 (0.40)	28
3,5-Ara*f*	9 (0.22)	6.0	8 (0.20)	6
4-Rha*p*	1 (0.07)	1.0	1 (0.07)	1
T-Gal*f*	1 (0.10)	1.0	2 (0.27)	1
5-Gal*f*	5 (0.17)	5.5	13 (0.06)	9.5
6-Gal*f*	3 (0.8)	5.5	10 (0.04)	9.5
5,6-Gal*f*	4 (0.76)	2.0	3 (0.01)	2

[a] Mole percent from GC/MS analysis is converted to moles per 59 mol (using total AG residues Table 1).
[b] Mole percent from GC/MS analysis is converted to moles per 79 mol (using total AG residues Table 1).

culosis AG (*M. leprae* with 56 and 83% the amount of *M. tuberculosis* for galactofuranose and arabinofuranose, respectively). Otherwise, the polymers are quite similar by linkage composition, which suggests a similar branching structure. To confirm this, the arabinan chains present on the *M. leprae* cell wall core were treated with a partially purified endo-arabinase enzyme, from *M. smegmatis* (15). The released oligo-arabinans were purified on a P-2 sizing column (16) into fractions poor and rich in galactosamine, which were analyzed by MALDI-TOF MS (Figs. 2 and 3 respectively). Although the endogenous arabinase prefers the α-1,5 cleavage of the residue in front of a branching point (16), it also cuts at various positions on the α-5-linked arabinan, resulting in multiple cleavages forming different sizes of arabinans as evident by MALDI-TOF spectra (Figs. 2 and 3). MALDI-TOF MS of the nongalactosaminylated per-*O*-acetylated arabinans identified a pattern of arabinans ranging from Ara_5 to Ara_{21}, with Ara_7 being the most predominant (Fig. 2*A*) and Ara_{18} being the dominant high molecular weight oligoarabinan. The lack of Ara_4 suggests that in the *M. leprae* arabinan the nonreducing terminus is fully branched (*i.e.* the pentaarabinoside shown in Figs. 2 and 3) like that of *M. tuberculosis* (16). Also very small amounts of arabinosyl oligomers from Ara_{14-17} are found in *M. leprae*, as is the case for *M. tuberculosis* (16), because of the enzyme's preference to only rarely cleave in long stretches of α-1,5 Ara*f* residues (16). For the same reason, oligomers of arabinose greater than Ara_{21} are also only

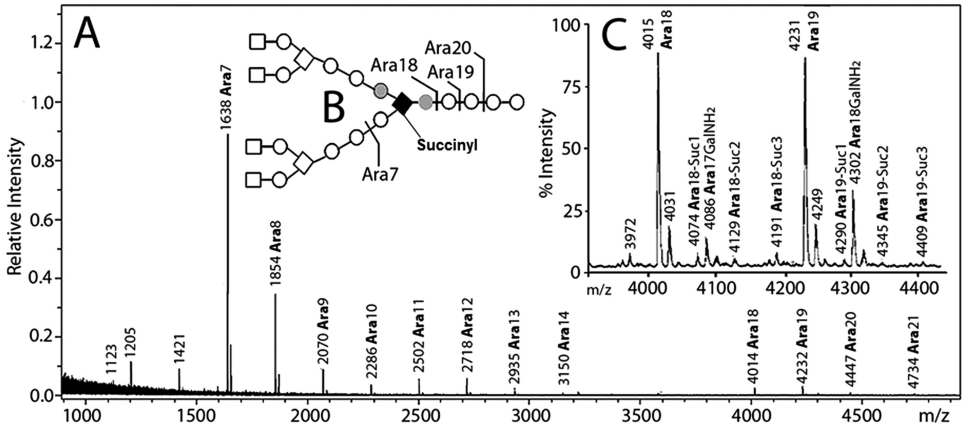

FIGURE 2. *A,* MALDI-TOF mass spectrum of predominantly nongalactosaminylated arabinans (after acetylation) released by endogenous arabinase from the cell wall core (mAGP) of *M. leprae*. Both $M + Na^+$ and, at 16 atomic mass units higher, $M + K^+$ ions are seen. The major species released are Ara_7, Ara_{18}, and Ara_{19} that are formed as illustrated in *B*. *C,* expansion of the spectrum from *m/z* 3900 to *m/z* 4500 showing the presence of 1–3 succinyl groups on Ara_{18} and Ara_{19}. Also seen are the galactosaminylated arabinans for Ara_{18} and Ara_{19} as the galactosaminylated and nongalactosaminylated arabinans were not perfectly separated from each other.

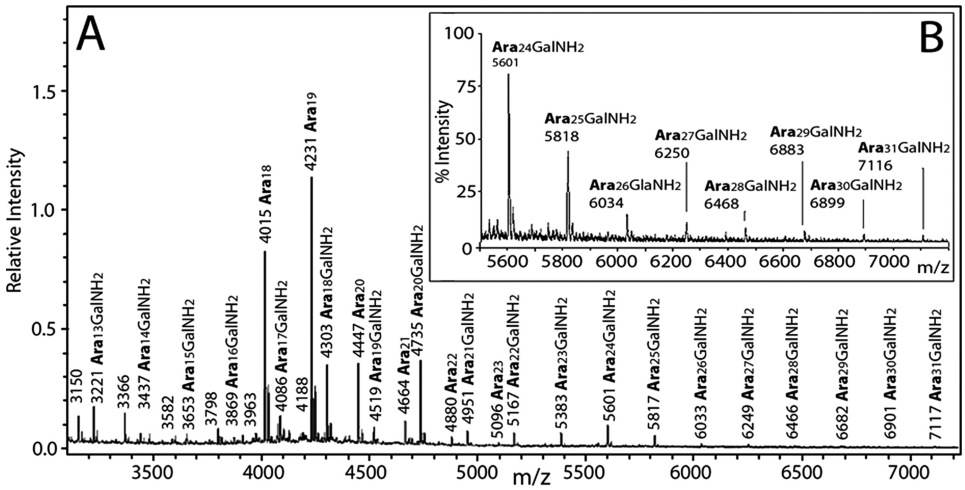

FIGURE 3. *A,* MALDI-TOF mass spectrum of the fraction enriched in galactosaminylated arabinans (after acetylation) released by endogenous arabinase from the cell wall core (mAGP) of *M. leprae*. Both $M + Na^+$ and, at 16 atomic mass units higher, $M + K^+$ ions are seen. The galactosaminylated species released are a series running from $Ara_{17}GalNH_2$ through $Ara_{31}GalNH_2$. *B,* expansion of the spectrum from *m/z* 5500 to *m/z* 7200 showing more clearly $Ara_{24}GalNH_2$ through $Ara_{31}GalNH_2$. The fragments are formed as in the illustration shown in Fig. 2*B* except succinyl is replaced by $GalNH_2$.

rarely formed; however, these arabinosyl oligomers, if detected, give information on how long are the internal arabinan chains linking the branched region to the galactan. Unlike the case with *M. tuberculosis*, we could not find nongalactosaminylated arabinans in *M. leprae* with a degree of polymerization greater than Ara_{21}; in *M. tuberculosis* up to Ara_{30} was found. However, such fragments are weak in *M. tuberculosis,* and one cannot be sure if this reflects an actual change in structure, especially because the more easily ionized $Ara_{31}GalNH_2$ was found in *M. leprae* (Fig. 3 and see below).

Careful examination of the expanded spectra of Fig. 2*B* revealed the presence of succinyl groups on the arabinan chains of *M. leprae*. The succinyl groups are 58 mass units heavier than the respective nonsuccinylated arabinans (M + 58) and, as in the cell wall of *M. tuberculosis* (16), multiple succinylation was observed. However, all ions resulting from succinylation were present at a much less intensity in the case of *M. leprae* (Fig. 2*B*). Succinylation was not observed in the galactosaminylated arabinans, a feature that was first observed in *M. tuberculosis* (16).

A direct analysis for succinyl groups in mAGP prepared from *M. leprae* was performed by GC/MS analysis after octanolysis of the cell wall to form succinyl dioctyl esters (10, 16). GC/MS analysis led to the identification of a peak that co-eluted with authentic dioctyl succinate and gave an identical mass spectrum ($[M + H]^+$ at *m/z* 343 and fragment ions at 213 and 231). Quantitation of succinyl residues indicated the molar ratio of succinyl residues to arabinosyl residues to be 1:175. Thus, the succinylation *in M. leprae* AG was 4.4-fold less than that of *M. tuberculosis* where the ratio of succinyl to arabinosyl residues was 1:41 (16) in agreement with the mass spectral data presented in Fig. 2.

The MALDI-TOF MS analyses of the endogenous arabinase released arabinans revealed that the smaller arabino-oligosaccharide fragments such as Ara_{7-8} did not show any succinylation (Fig. 2). This observation implies that the succinates are probably located on the internal α-3,5-arabinan chain, as in *M. tuberculosis,* although definitive data such as NMR done for *M. tuberculosis* (16) are lacking.

The MALDI-TOF spectrum of the arabinans containing a $GalNH_2$ residue is presented in Fig. 3. In this case, oligoarabinosides up to $Ara_{31}(GalNH_2)_1$ are seen, exactly as was found for *M. tuberculosis* arabinan (16). Their presence, in contrast to the lack of nongalactosaminylated arabinans containing greater than 21 residues (Fig. 2), may be due to MS detection issues as the $GalNH_2$ residue allows for stronger ionization or it may reflect a genuine difference in arabinan elongation. No succinyl groups are present on the $GalNH_2$-substituted arabinans in *M. leprae* as in *M. tuberculosis* (16). The reason for this is likely that both the first succinyl and the $GalNH_2$ are attached to the 2-position of the interior branched 3,5-Ara*f*.

Data from *C. glutamicum* suggest that up to three arabinans can be attached per galactan chain (17). We had assumed the same number for mycobacteria (16), but the presence of three arabinan chains does not fit the data of Table 1 or 2 for either *M. tuberculosis* or *M. leprae.* For *M. tuberculosis*, the glycosyl composition data of Table 1 suggest about 53 arabinosyl residues per AG molecule. The MS analysis contained $M + Na^+$ ions for galactosaminylated arabinosides only up to Ara_{31} suggesting the lack of arabinans longer than Ara_{31}. Thus, two arabinans with an average of 26 arabinosyl residues are most likely present. For *M. leprae,* the glycosyl linkage data (Table 2) require about 45 arabinosyl residues, which is consistent with two arabinans averaging 22 arabinosyl residues each. In both cases, the data suggest heterogeneity in the length of the α-1,5-Ara*f* linear interior region of the arabinan. One possible caveat is the presence of more branched 5,6-Gal*f* in both cases than expected, as indicated in Table 2. It is possible that additional α-1,5-Ara*f* linear arabinan chains with no Ara_{17} branched reducing end, perhaps only one or two Ara*f* units long, are also present.

Attachment of Mycolic Acids to the Arabinan Chains—Previous data from *M. tuberculosis*, using selective alkylation of arabinan (14), revealed that approximately two-thirds of the sites for mycolate attachment (C-5 of the T-Ara*f* and C-5 of the 2-Ara*f* as depicted in Figs. 2 and 3) were occupied with mycolate residues. This is consistent with the data presented in Table 1 where a fully substituted AG molecule with two arabinans (in the case of *M. tuberculosis*) has 16 potential sites for mycolylation, and if two-thirds are occupied, the ratio of AG to mycolate would be 1:10.7, which is reasonably consistent with the found ratio of 1:12.6 or 79% occupied (Table 1). For *M. leprae,* Table 1 reveals a ratio of AG to mycolate of one AG molecule for every 6.9 mycolic acids or 42% of the possible mycolylation sites being occupied. However, as shown in Table 1, in the wall of *M. leprae* there are considerably more AG molecules per 10 PG repeating units (3.0 *versus* 1.3 as shown in Table 1), and thus the ratio of mycolate to PG is higher in *M. leprae* (20.8 mycolates/10 PG repeat units) than in *M. tuberculosis* (16.4 mycolates/10 PG repeat units) even though the arabinans themselves are not as fully substituted.

The AG, in turn, is attached to the peptidoglycan. In the case of *M. tuberculosis* AG, our data calculate to one AG molecule per eight disaccharide repeat units of PG (Table 1), which agrees reasonably well with earlier work (13, 30). In the case of the more abundant AG molecules in *M. leprae,* our data calculate to one AG molecule for every 3.3 repeat units of PG (Table 1).

DISCUSSION

Primary Structural Considerations—The PG of *M. leprae* differs from the PG of *M. tuberculosis* only by the lack of *N*-glycolylated muramic acid in its peptidoglycan and the substitution of glycine for L-alanine (11). Our results show that the AG structures of *M. tuberculosis* and *M. leprae* are similar with each AG molecule containing ~79 and 59 glycosyl residues, respectively. The galactan is consistently shorter in *M. leprae* than in *M. tuberculosis* (13 *versus* 23 residues). The basic architecture of the arabinan is the same with a doubly branched structure as shown by the data in Figs. 2 and 3. The composition and methylation data fit best with approximately two arabinan chains per AG molecule in both *M. tuberculosis* and *M. leprae* AG (Tables 1 and 2), but the chains are shorter in *M. leprae*. One of the largest differences between the two species is that more AG molecules are present per PG molecule in the *M. leprae* cell wall (3.0 AG molecules/10 repeating units of PG) than in *M. tuberculosis* (1.3 AG molecules/10 repeating units of PG) with a *p* value of less than 0.001 in the Tukey-Kramer *t* test comparing the two ratios. Thus, the cell wall of *M. leprae* is poised for a higher degree of mycolylation and indeed does have a higher degree of mycolylation per 10 repeating units of PG (20.8 for *M. leprae versus* 16.4 for *M. tuberculosis*) with a *p* value of less than 0.05 in the Tukey-Kramer *t* test comparing the two ratios. The fact that the AG molecules are somewhat shorter in *M. leprae* may result in a smaller periplasmic space.

Modeling the Mycobacterial Cell Wall—Recent innovations of the conformation of mycolic acids and the packing of hydrocarbon chains allow modeling of the conformation of the mycolates as they are attached to AG. Thus, two studies using cryo-electron microscopy have shown that the inner half of the outer membrane of mycobacteria is consistent with the mycolic acids occurring in a folded configuration (18, 19). Earlier and independently, Villeneuve *et al.* (31, 32) also proposed a folded mycolic acid structure based on Langmuir monolayer packing. They proposed that essentially four columns are present that are not in a single plane, but rather they extend outward from the apexes of a parallelogram as shown in Fig. 4, *B* and *D* (32). A lipid bilayer of C-20 fatty acids revealed unit cell dimensions of 5.8×4.1 Å when analyzed by scanning tunneling microscopy (34), suggesting similar dimensions for each mycolate column (Fig. 4*D*).

The structure of the arabinan and the confirmation of the mycolic acid present considerable steric restraints. Thus, given the ~5-Å size of a mycolate column and the molecular dimensions of the terminal pentaarabinoside, the attachment of four mycolates can only take place in a unique conformation of the mycolates and the terminal pentaarabinoside as illustrated in Fig. 4, *B–D*. This is because the primary hydroxyl groups on the T-Ara*f* and the 2-Ara*f* groups can only be spaced 5–8 Å apart as shown clearly with molecular models. Because each mycolate molecule carries four columns with it, the pentaarabinoside cannot be in a linear arrangement as the mycolate columns will interfere with each other, but it must be as shown in Fig. 4*C* leading to the mycolates adopting a conformation similar to that shown in Fig. 4*B*. The overall arrangement is shown in Fig. 4*D*.

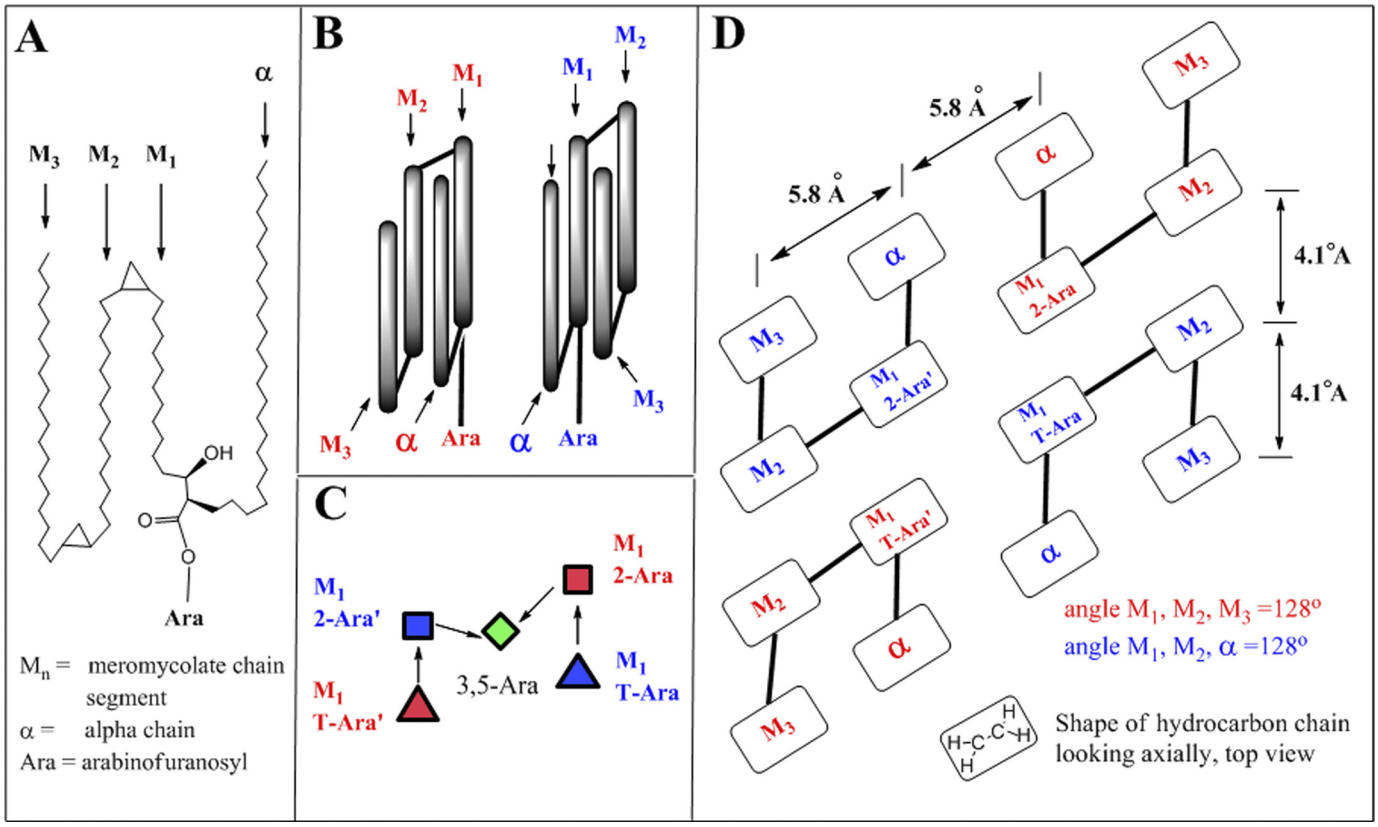

FIGURE 4. *A,* two-dimensional representation of an α-mycolic acid folded to form four hydrocarbon domains. Three of these domains, M1, M2, and M3, are in the meromycolate portion of the molecule, and one, labeled "α," is the α chain region of the molecule. The esterification to the 5-position of either the β-T-Ara*f* or the α-2-Ara*f* at the carboxyl group between the α and M1 domain is also shown. *B,* three-dimensional representation of two α-mycolic acids folded to form four hydrocarbon domains each. The conformation designated with *red* and *blue labeling* are, at the level of the four chains, mirror images, and both conformations are needed to fit the mycolates onto the arabinan (as shown in *C* and *D*). *C,* approximate conformation the nonreducing terminal pentaarabinosyl unit must adopt to accommodate complete mycolic acid substitution. The pentaarabinosyl unit is viewed from the top; the two T-Ara and the two 2-Ara are residues are roughly in the same vertical plane, and the 3,5-Ara unit is below them. The colored symbols representing the arabinosyl residues correlate to the two conformations shown in *B*. *D,* schematic top view of a tetramycolylated nonreducing terminal pentaarabinosyl unit.

In addition, the data of Tables 1 and 2 can be used to estimate what percentages of the fatty acyl groups in the inner leaflet of the outer membrane are mycolic acids covalently linked to AG and thus what percentage of the PG surface area is covered with mycolic acids covalently linked to it (via AG). Thus (see Table 3), it is reasonable to assume that the four columns of each mycolate when viewed from above cover about 95 Å^2 given their four-column structure (32) and the dimensions of a single fatty acid chain of 19.4 Å^2 (34). To calculate the area of the PG, its orientation to the cell must be known as well as the dimensions of the glycan and connecting peptides. A consensus is emerging that PG glycan strains are mostly circumferential (35), that the peptide cross-links are not fully extended (36), and that in Gram-negative bacteria (and by implication in mycobacterial PG) there is only a single layer of PG present, parallel to the plasma membrane (35, 36). Quantitative analysis of PG and the surface area in *E. coli* suggests that the unit cell of PG (disaccharide repeat with its half of a connecting peptide cross-link) has an area of 250 Å^2 in one study (36) and 170 Å^2 in an earlier study (37). In contrast, direct visualization of the PG glycan chains by electron cryotomography suggested separation of the glycan chains by 50–80 Å (35). (Separation by greater than 52 Å is beyond the theoretical limit if the glycans are perfectly parallel, which they may not be (38).) Using these

TABLE 3

Calculated percent coverage of the PG layer by the mycolate layer for *M. leprae* and *M. tuberculosis* cell wall at different PG conformations

Mycolate dimension	(5.8 Å by 4.1Å 128° parallelogram)[a]		(5.8 Å by 4.1Å 128° parallelogram)[a]		(5.8 Å by 4.1Å 128° parallelogram)[a]	
Mycolate area	95 (Å^2)[b]		95 (Å^2)		95 (Å^2)	
PG Orientation	Horizontal		Horizontal		Horizontal	
PG layers	1[c]		1		1	
PG disaccharide unit area	250 (Å^2)[d]		170 (Å^2)[e]		520 (Å^2)[f]	
PG Dimensions	10 Å[g] by 25 Å		10 Å[g] by 17 Å		10 Å[g] by 52 Å[f]	
Calculated ratio Myc/PG disaccharide unit at full coverage	2.6 (250/95)		1.8 (170/95)		5.5 (520/95)	
	M. Tb	M. Lep	M. Tb	M. Lep	M. Tb	M. Lep
Experimental Myc/PG ratio	1.64	2.08	1.64	2.08	1.64	2.08
% Coverage of PG layer by Mycolates	63%	80%	91%	115%	30%	38%

[a] Data are based on measurement for C-20 fatty acids by tunneling microscopy (34).
[b] Data are calculated from mycolate dimensions and are reasonably consistent with studies on Langmuir monolayers (31), which yields 78 Å^2 for four chains.
[c] Data are based on electron cryotomography in *E. coli* (35).
[d] Data indicate the measured area in *E. coli* (37).
[e] Data indicate the measured area in a different strain of *E. coli* (38).
[f] 52 Å is the distance of a fully extended peptide chain and the associated glycan (39); glycan chains (which may not be perfectly parallel) were found to be 50–80 Å apart by electron cryotomography (35).
[g] Data are calculated from the known 10 Å disaccharide length.

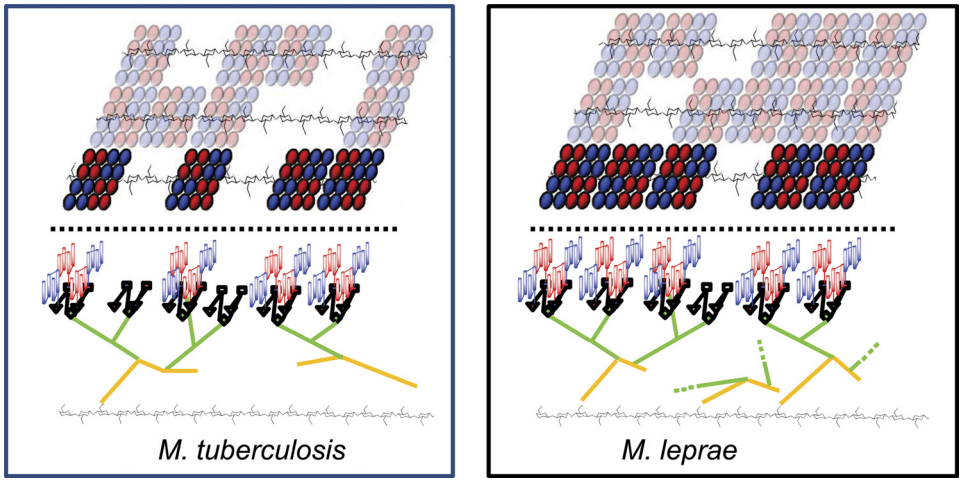

FIGURE 5. ***Left,* model of *M. tuberculosis* cell wall; *right,* model of *M. leprae* cell wall.** Top portion of figures (*above dashed line*) shows an arrangement of the covalently bound mycolates present in the inner leaflet of the outer membrane as viewed looking down at the cell wall. The peptidoglycan beneath the mycolates is shown, but the connecting AG is not. The orientation of PG *versus* the mycolates is arbitrary; the flexibility of the AG would allow any orientation. The positions of the "blank" areas devoid of covalently linked mycolates are also arbitrary, but the percent coverage of the PG layer is ~63% for *M. tuberculosis* and ~80% for *M. leprae* (see Table 3). The blank areas are presumably filled with noncovalently attached lipids such as trehalose mono- and di-mycolates. Bottom portion of figures (*below dashed line*) show a side view of the mycolates attached to PG for the mycolate clusters in bright colors shown in the top view. The PG is shown in *black* with only the GlcNAc-MurNAc repeat units designated. The AG is shown in *gold* (galactan) and *green* (arabinan). The nonreducing pentaarabinoside is shown with *diamonds, squares,* and *triangles* as in Fig. 4*C*. The mycolates are as shown in Fig. 4, *B* and *D,* but are not in scale with the rest of the drawing; rather they are shown much smaller for clarity.

different areas for the disaccharide unit surfaces areas, the coverage of the PG layer varies from 29 to 88% for *M. tuberculosis* and from 39 to 119% for *M. leprae* (Table 3). Clearly, more precise data on the area of the PG monomers are required, but in all estimates, even with the larger PG monomeric unit, a substantial portion of the inner leaflet is covalently attached to mycolic acids in contrast to typical Gram-negative bacteria where only a few percent of the fatty acyl groups of the inner leaflet of the outer membrane are covalently attached to PG via the cell wall lipoprotein.

A model of the covalently attached mycolate "patches" assuming a PG unit area of 250 $Å^2$ (~63% PG coverage for *M. tuberculosis* and 80% PG coverage for *M. leprae*) is shown in Fig. 5. The empty regions are presumably filled with noncovalently attached lipids such as trehalose mono- and di-mycolates. The structure of a single arabinan is such that the two "outer arms" can readily accommodate mycolate patches that are next to each other or as far apart as 45 Å. Some attempt was made for proper scaling. Thus, one AG molecule for eight PG repeat units is shown for *M. tuberculosis,* whereas three AG molecules per 10 AG repeat units is shown for the *M. leprae* cell wall (see Table 1). Also, approximately 79% of the AG from *M. tuberculosis* is substituted with mycolic acids as compared with 42% for *M. leprae* (Table 1). It is readily apparent that the AG from *M. leprae* is more abundant (*i.e.* more molecules per PG repeating unit) and also that the AG is capable of accepting additional mycolic acid groups.

The conversion of *M. tuberculosis* from an actively growing acid-fast form to a nonactively growing non-acid-fast form during the course of infection is well documented (2). Although the mechanism of acid-fastness is subtle and not understood, it is clear that a change in cell wall must occur in the nongrowing *M. tuberculosis*. The difference between the cell walls of *M. leprae* grown *in vivo versus M. tuberculosis* grown *in vitro* suggests that a possible change might be the presence of additional AG molecules and covalently linked mycolic acids rendering these bacteria less permeable in general. Clearly what is required at this stage is a careful analysis of acid fast *M. tuberculosis* cell walls isolated from animals during logarithmic growth and comparison to the non-acid-fast bacilli evident during the dormancy phase of tuberculosis; such studies are in progress.

Acknowledgments—We gratefully acknowledge Dr. John Spencer for providing the M. leprae cell wall core via National Institutes of Health NIAID Contract AI 25469 and Dr. Alan Schenkel for help with statistical analysis.

REFERENCES

1. Crick, D. C., Brennan, P. J., and McNeil, M. R. (2004) in *Tuberculosis* (Rom, W. N., and Garay, S. M., eds) pp. 115–134, Lippincott Williams & Wilkins, Philadelphia
2. Seiler, P., Ulrichs, T., Bandermann, S., Pradl, L., Jörg, S., Krenn, V., Morawietz, L., Kaufmann, S. H., and Aichele, P. (2003) *J. Infect. Dis.* **188,** 1326–1331
3. Vijayaraghavan, R. (2009) *Scand. J. Lab. Anim. Sci.* **36,** 167–176
4. Levy, L. (1976) *Lepr. Rev.* **47,** 103–106
5. Ordway, D., Henao-Tamayo, M., Harton, M., Palanisamy, G., Troudt, J., Shanley, C., Basaraba, R. J., and Orme, I. M. (2007) *J. Immunol.* **179,** 522–531
6. Muñoz-Elías, E. J., Timm, J., Botha, T., Chan, W. T., Gomez, J. E., and McKinney, J. D. (2005) *Infect. Immun.* **73,** 546–551
7. Cummins, C. S., Atfield, G., Rees, R. J., and Valentin, R. C. (1967) *J. Gen. Microbiol.* **49,** 377
8. David, H. L., and Rastogi, N. (1983) *Curr. Microbiol.* **9,** 269–274
9. Draper, P., Kandler, O., and Darbre, A. (1987) *J. Gen. Microbiol.* **133,** 1187–1194
10. Torrelles, J. B., Khoo, K. H., Sieling, P. A., Modlin, R. L., Zhang, N., Marques, A. M., Treumann, A., Rithner, C. D., Brennan, P. J., and Chatterjee, D. (2004) *J. Biol. Chem.* **279,** 41227–41239
11. Mahapatra, S., Crick, D. C., McNeil, M. R., and Brennan, P. J. (2008) *J. Bacteriol.* **190,** 655–661
12. Daffe, M., Brennan, P. J., and McNeil, M. (1990) *J. Biol. Chem.* **265,** 6734–6743

13. McNeil, M., Daffe, M., and Brennan, P. J. (1990) *J. Biol. Chem.* **265,** 18200–18206
14. McNeil, M., Daffe, M., and Brennan, P. J. (1991) *J. Biol. Chem.* **266,** 13217–13223
15. Dong, X., Bhamidi, S., Scherman, M., Xin, Y., and McNeil, M. R. (2006) *Appl. Environ. Microbiol.* **72,** 2601–2605
16. Bhamidi, S., Scherman, M. S., Rithner, C. D., Prenni, J. E., Chatterjee, D., Khoo, K. H., and McNeil, M. R. (2008) *J. Biol. Chem.* **283,** 12992–13000
17. Alderwick, L. J., Radmacher, E., Seidel, M., Gande, R., Hitchen, P. G., Morris, H. R., Dell, A., Sahm, H., Eggeling, L., and Besra, G. S. (2005) *J. Biol. Chem.* **280,** 32362–32371
18. Hoffmann, C., Leis, A., Niederweis, M., Plitzko, J. M., and Engelhardt, H. (2008) *Proc. Natl. Acad. Sci. U.S.A.* **105,** 3963–3967
19. Zuber, B., Chami, M., Houssin, C., Dubochet, J., Griffiths, G., and Daffé, M. (2008) *J. Bacteriol.* **190,** 5672–5680
20. Hunter, S. W., Rivoire, B., Mehra, V., Bloom, B. R., and Brennan, P. J. (1990) *J. Biol. Chem.* **265,** 14065–14068
21. Ciucanu, I., and Kerek, F. (1984) *Carbohydr. Res.* **131,** 209–217
22. Sweet, D. P., Shapiro, R. H., and Albersheim, P. (1975) *Carbohydr. Res.* **40,** 217–225
23. Amar-Nacasch, C., and Vilkas, E. (1970) *Bull. Soc. Chim. Biol.* **52,** 145–151
24. Shui, G., Bendt, A. K., Pethe, K., Dick, T., and Wenk, M. R. (2007) *J. Lipid Res.* **48,** 1976–1984
25. Song, S. H., Park, K. U., Lee, J. H., Kim, E. C., Kim, J. Q., and Song, J. (2009) *J. Microbiol. Methods* **77,** 165–177
26. Minnikin, D. E., Dobson, G., Goodfellow, M., Draper, P., and Magnusson, M. (1985) *J. Gen. Microbiol.* **131,** 2013–2021
27. Kusaka, T., and Mori, T. (1986) *J. Gen. Microbiol.* **132,** 3403–3406
28. Watanabe, M., Aoyagi, Y., Mitome, H., Fujita, T., Naoki, H., Ridell, M., and Minnikin, D. E. (2002) *Microbiology* **148,** 1881–1902
29. Minnikin, D. E., and Polgar, N. (1967) *Chem. Commun.* **18,** 916–918
30. Cunto, G., Kanetsuna, F., and Imaeda, T. (1969) *Biochim. Biophys. Acta* **192,** 358–360
31. Villeneuve, M., Kawai, M., Kanashima, H., Watanabe, M., Minnikin, D. E., and Nakahara, H. (2005) *Biochim. Biophys. Acta* **1715,** 71–80
32. Villeneuve, M., Kawai, M., Watanabe, M., Aoyagi, Y., Hitotsuyanagi, Y., Takeya, K., Gouda, H., Hirono, S., Minnikin, D. E., and Nakahara, H. (2007) *Biochim. Biophys. Acta* **1768,** 1717–1726
33. Deleted in proof
34. Smith, D. P., Bryant, A., Quate, C. F., Rabe, J. P., Gerber, C., and Swalen, J. D. (1987) *Proc. Natl. Acad. Sci. U.S.A.* **84,** 969–972
35. Gan, L., Chen, S., and Jensen, G. J. (2008) *Proc. Natl. Acad. Sci. U.S.A.* **105,** 18953–18957
36. Wientjes, F. B., Woldringh, C. L., and Nanninga, N. (1991) *J. Bacteriol.* **173,** 7684–7691
37. Zaritsky, A., Woldringh, C. L., and Mirelman, D. (1979) *FEBS Lett.* **98,** 29–32
38. Vollmer, W., and Höltje, J. V. (2004) *J. Bacteriol.* **186,** 5978–5987
39. Dmitriev, B. A., Toukach, F. V., Schaper, K. J., Holst, O., Rietschel, E. T., and Ehlers, S. (2003) *J. Bacteriol.* **185,** 3458–3468
40. Sartain, M. J., Dick, D. L., Rithner, C. D., Crick, D. C., and Belisle, J. T. (2011) *J. Lipid Res.* **52,** 861–872